Effect of Osmolytes on the Binding of EGR1 Transcription Factor to DNA

David C. Mikles, Vikas Bhat, Brett J. Schuchardt, Caleb B. McDonald, Amjad Farooq

Department of Biochemistry and Molecular Biology, Leonard Miller School of Medicine, University of Miami, Miami, FL 33136

ABSTRACT:

Osmolytes play a key role in maintaining protein stability and mediating macromolecular interactions within the intracellular environment of the cell. Herein, we show that osmolytes such as glycerol, sucrose, and polyethylene glycol 400 (PEG400) mitigate the binding of early growth response (protein) 1 (EGR1) transcription factor to DNA in a differential manner. Thus, while physiological concentrations of glycerol only moderately reduce the binding affinity, addition of sucrose and PEG400 is concomitant with a loss in the binding affinity by an order of magnitude. This salient observation suggests that EGR1 is most likely subject to conformational equilibrium and that the osmolytes exert their effect via favorable interactions with the unliganded conformation. Consistent with this notion, our analysis reveals that while EGR1 displays rather high structural stability in complex with DNA, the unliganded conformation becomes significantly destabilized in solution. In particular, while liganded EGR1 adopts a well-defined arc-like architecture, the unliganded protein samples a comparatively large conformational space between two distinct states that periodically interconvert between an elongated rod-like shape and an arc-like conformation on a submicrosecond time scale.

Correspondence to: Amjad Farooq; e-mail: amjad@farooqlab.net

Consequently, the ability of osmolytes to favorably interact with the unliganded conformation so as to stabilize it could account for the negative effect of osmotic stress on EGR1–DNA interaction observed here. Taken together, our study sheds new light on the role of osmolytes in modulating a key protein–DNA interaction. © 2014 Wiley Periodicals, Inc. Biopolymers 103: 74–87, 2015.

Keywords: protein–DNA thermodynamics; osmotic stress; conformational; equilibrium; molecular dynamics

INTRODUCTION

Osmolytes are small organic molecules that are naturally found within the intracellular environment of living organisms, where they exert protective functions against extreme environmental conditions and osmotic stress.[1] Examples include amino acids and their derivatives (such as glycine, proline, and taurine), polyols and sugars (such as glycerol, sucrose, and trehalose), and methylamines [such as trimethylglycine (betaine) (TMG), *N*-methylyglycine (sarcosine) (NMG), and trimethylamine *N*-oxide (TMAO)].[2,3] In particular, osmolytes play a key role in maintaining cellular homeostasis by virtue of their ability to not only regulate cell volume but also stabilize and protect macromolecules from the physical stress and denaturing conditions inherent to life.[4–12] More importantly, osmolytes are also believed to displace water from interacting surfaces,
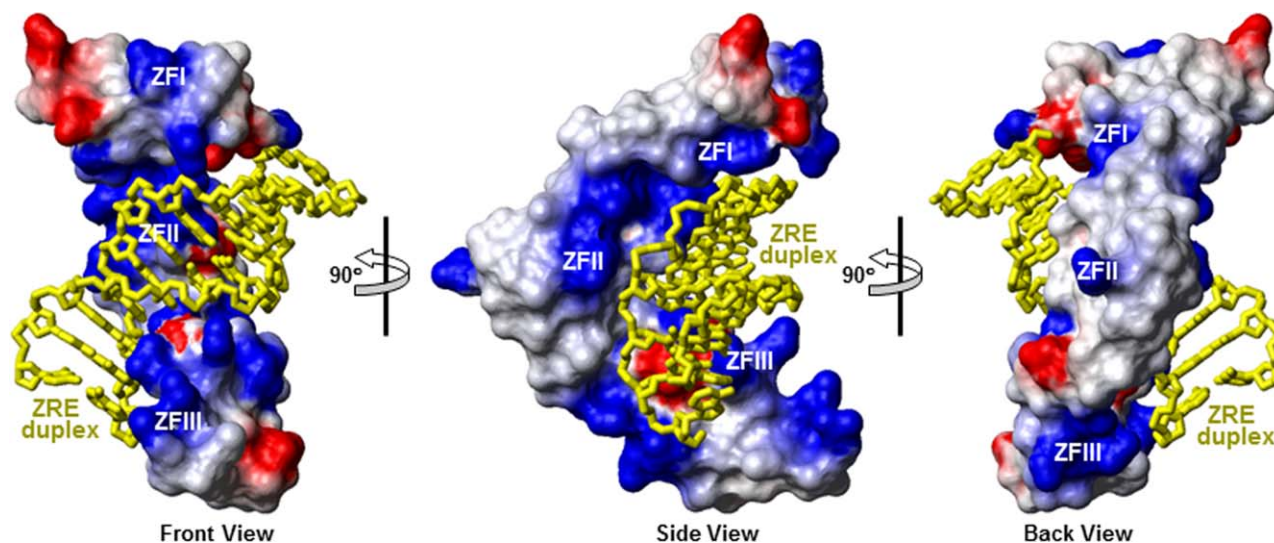
FIGURE 1 Electrostatic surface potential map derived from the structural model of the DB domain of EGR1 in complex with ZRE duplex. The relative location of three tandem zinc fingers (denoted ZFI, ZFII, and ZFIII) is indicated on the composite molecular surface of the DB domain. Note that three different orientations of the DB domain, related by a 90°-clockwise rotation about the vertical axis in successive order from left to right, are shown for the inquisitive eye. The blue and red colors, respectively, denote the density of positive and negative charges, while the apolar and polar surfaces are indicated by white/gray color on the molecular surface. The ZRE duplex is displayed as a "stick" model and colored yellow.

binding clefts, active sites and other cavities found within macromolecules and, in so doing, aid ligand binding to proteins and enhance enzymatic activity. In general, such dehydration of molecular surfaces positively correlates with the ability of many osmolytes to promote folding of proteins and augment protein stability through their unfavorable interactions with the unfolded state.[13–17] However, destabilizing effects of osmolytes on protein structure have also been recently noted.[18–21]

In an effort to further our understanding of the role of osmolytes in mediating macromolecular functions, we undertook the present study on the binding of human early growth response (protein) 1 (EGR1) transcription factor, also known as Zif268, to its cognate DNA. Briefly, EGR1 is constructed on the classical TA-DB modular design, where the TA is the N-terminal transactivation domain and DB is the C-terminal DNA-binding domain.[22–24] Upon activation in response to extracellular stimuli—such as hormones, neurotransmitters, and growth factors—EGR1 binds via its DB domain to the promoters of target genes containing the GCGTGGGCG consensus motif, referred to hereinafter as Zif268 response element (ZRE), in a sequence-dependent manner.[25,26] The resulting EGR1–DNA interaction facilitates the TA domain to recruit a diverse array of transcriptional co-regulators to cognate DNA promoters and, in so doing, plays a key role in modulating the transcriptional machinery. Importantly, EGR1 couples extracellular stimuli to changes in gene expression responsible for a myriad of cellular activities ranging from cell growth and proliferation to apoptosis and oncogenic transformation.[27–30] It should be noted here that the DB domain of EGR1 is comprised of three tandem copies of C2H2-type zinc fingers (ZF), designated herein ZFI, ZFII and ZFIII, which come together in space to assemble into an arc-like architecture that snugly fits into the major grooves of DNA (Figure 1). Of particular note is the observation that the solvent-accessible surface of the DB domain is bolstered by electrostatic polarization, with the inner face of the arc harboring an overall positive charge, while the outer rim is largely neutral. Such electrostatic polarization of the DB domain is not surprising given its role as a transcription factor—however, its arc-like conformation does not bode well for its structural integrity in isolation. Simply put, while the positively charged inner face appears to be a prerequisite for the ability of DB domain to establish a stable interaction with the negatively charged DNA, the rather highly constrained arc-like architecture will in all probability undergo some sort of structural rearrangement in the absence of DNA so as to minimize electrostatic repulsions between the three tandem zinc fingers. Given that the zinc fingers within the DB domain are held together by flexible "hinges," such conformational transition will not only be a thermodynamic necessity but also

dynamically feasible. Conversely speaking, the DB domain of EGR1 must experience a reverse conformational switching upon binding to DNA.

In light of the above-mentioned conformational equilibrium, we hypothesize that the osmolytes favorably interact with the unliganded conformation of EGR1 and, in so doing, tightly modulate the EGR1–DNA interaction by virtue of their ability to stabilize the unliganded protein relative to the liganded state. To test our hypothesis, we have employed here various biophysical methods to investigate the effect of natural osmolytes glycerol and sucrose as well as a widely used synthetic osmolyte polyethylene glycol (PEG) 400 (PEG400) on the binding of DB domain of EGR1 to DNA. Our analysis shows that these osmolytes mitigate the binding of EGR1 to DNA in a differential manner in agreement with our hypothesis. We discuss these findings in light of the ability of EGR1 to undergo conformational equilibrium.

MATERIALS AND METHODS

Protein Preparation

The DB domain (residues 331–430) of human EGR1 was cloned into pET30 bacterial expression vector with an N-terminal His-tag using Novagen ligation-independent cloning technology as described previously.[31] The recombinant protein was subsequently expressed in *Escherichia coli* BL21*(DE3) bacterial strain and purified on a Ni-NTA affinity column followed by size-exclusion chromatography (SEC) using standard procedures.[31] Final yield was typically between 5 and 10 mg protein of apparent homogeneity per liter of bacterial culture. Protein concentration was spectrophotometrically determined on the basis of an extinction coefficient of 12,865 $M^{-1}cm^{-1}$ calculated using the online software ProtParam at ExPasy Server.[32]

DNA Synthesis

15-mer DNA oligos containing the ZRE consensus site (GCGTGGGCG) were commercially obtained from Sigma Genosys. The complete nucleotide sequence of the sense and antisense oligos constituting the ZRE duplex is shown below:

5′-ataGCGTGGGCGttt-3′
3′-tatCGCACCCGCaaa-5′

Oligo concentrations were determined spectrophotometrically on the basis of their extinction co-efficients derived from their nucleotide sequences using the online software OligoAnalyzer 3.1. Equimolar amounts of sense and antisense oligos were mixed together and heated at 95°C for 10 min and then allowed to cool to room temperature to obtain double-stranded DNA (dsDNA)-annealed oligos (ZRE duplex).

ITC Measurements

Isothermal titration calorimetry (ITC) experiments were performed on a TA Nano-ITC instrument. Briefly, the DB domain of EGR1 and the ZRE duplex were dialyzed in 50 mM Sodium phosphate and 5 mM β-mercaptoethanol containing varying concen-

trations of glycerol, sucrose, or PEG400 at pH 7.0. All experiments were initiated by injecting 25 $\times$ 10 μl aliquots of 100–200 μM of ZRE duplex from the syringe into the calorimetric cell containing 0.95 ml of 10–20 μM of DB domain solution at 25°C. The change in thermal power as a function of each injection was automatically recorded using the integrated NanoAnalyze software. The raw data were further integrated to yield binding isotherms of heat release per injection as a function of molar ratio of ZRE duplex to DB domain. The heats of mixing and dilution were subtracted from the heat of binding per injection by carrying out a control experiment in which the same buffer in the calorimetric cell was titrated against the ZRE duplex in an identical manner. To determine the equilibrium dissociation constant (K_d) and the enthalpy change ($\Delta H°$) associated with the binding of DB domain to DNA in the absence and presence of varying concentrations of osmolytes, the binding isotherms were iteratively fit to a built-in one-site model by nonlinear least squares regression analysis using the integrated NanoAnalyze software as described previously.[31,33] The free energy change ($\Delta G°$) upon binding was calculated from the relationship:

$$\Delta G° = RT \ln K_d \qquad (1)$$

where R is the universal molar gas constant (1.99 cal/mol/K) and T is the absolute temperature (298 K). The entropic contribution ($T\Delta S°$) to the free energy of binding was calculated from the relationship:

$$T\Delta S° = \Delta H° - \Delta G° \qquad (2)$$

where $\Delta H°$ and $\Delta G°$ are as defined above.

Circular Dichroism

Circular dichroism (CD) measurements were conducted on a thermostatically-controlled Jasco J-815 spectropolarimeter. Briefly, samples of DB domain of EGR1 and ZRE duplex were individually prepared in 50 mM Sodium phosphate buffer containing varying concentrations of glycerol, sucrose, and PEG400 at pH 7.0. For the DB domain, far-UV spectral measurements were conducted on 10 μM of protein in the 195–255 nm wavelength range at 25°C. For the ZRE duplex, UV spectral measurements were conducted on 10 μM of dsDNA oligo in the 200–320 nm wavelength range at 25°C. All data were collected using a quartz cuvette with a 2-mm pathlength and recorded with a slit bandwidth of 2 nm at a scan rate of 10 nm/min and normalized against reference spectra to remove the background contribution of buffer. Each spectral dataset represents an average of four scans acquired at 0.1 nm intervals. For thermal scans of the DB domain, the spectral intensity at a wavelength of 222 nm ($[\theta_{222}]$) was monitored in the temperature range 20–90°C at a scan rate of 1°C/min. All data were converted to mean ellipticity, $[\theta]$, as a function of wavelength (λ) of electromagnetic radiation using the equation:

$$[\theta] = [(10^5 \Delta e)/cl] \text{ deg.cm}^2.\text{dmol}^{-1} \qquad (3)$$

where $\Delta\varepsilon$ is the observed ellipticity in mdeg, c is the protein concentration in μM, and l is the cuvette pathlength in cm.

Molecular Modeling

Molecular modeling (MM) was employed to build a structural model of the DB domain of EGR1 in complex with the 15-mer ZRE duplex
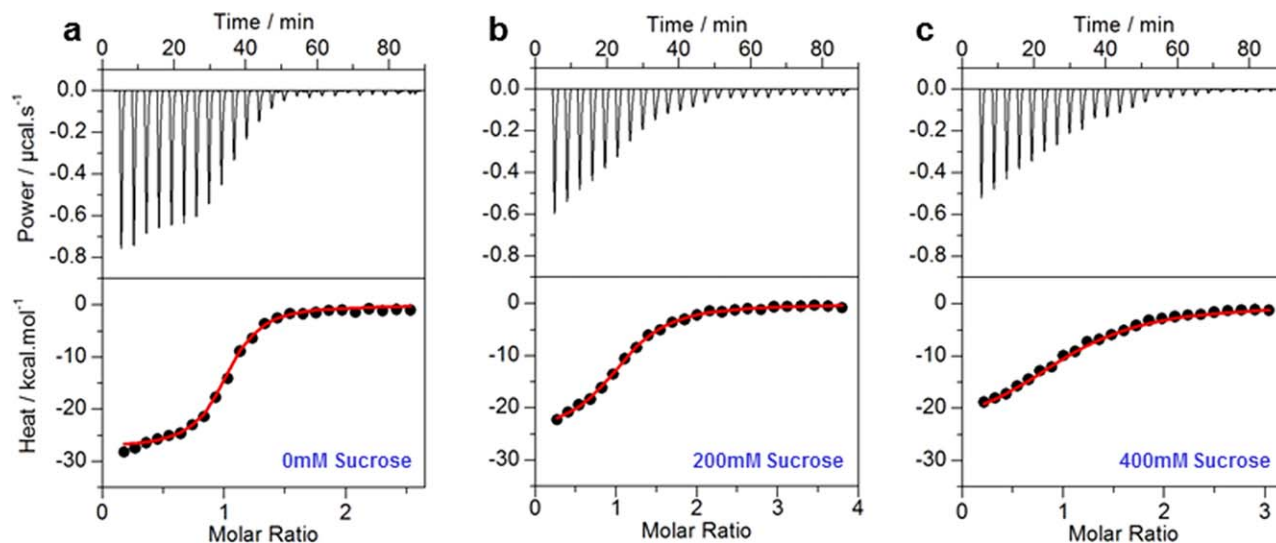
FIGURE 2   Representative ITC isotherms for the binding of ZRE duplex to DB domain of EGR1 at sucrose concentrations of 0 mM (a), 200 mM (b), and 400 mM (c). The upper panels show raw ITC data expressed as change in thermal power with respect to time over the period of titration. In the lower panels, change in molar heat is expressed as a function of molar ratio of ZRE duplex to DB domain. The red solid lines in the lower panels show the fit of data to a one-site binding model using the integrated NanoAnalyze software as described previously.[31,33]

using the corresponding crystal structure determined by Pavletich and Pabo[26] in the MODELLER software[34] as described earlier.[31] A total of 100 structural models were calculated and the structure with the lowest energy, as judged by the MODELLER Objective Function, was selected for further analysis. The electrostatic surface potential map of the structural model was generated using MOLMOL.[35] The unliganded structural model of DB domain was generated simply by stripping away atomic coordinates of DNA from the liganded protein. It was assumed that the DB domain underwent no structural change upon binding to DNA in a rigid body fashion (an assumption that would eventually prove to be incorrect but it nonetheless did serve the desired purpose).

Molecular Dynamics

Molecular dynamics (MD) simulations on the structural models of the DB domain of EGR1 bound to DNA (liganded) and in the absence of DNA (unliganded) were performed with the GROMACS software[36,37] using the integrated AMBER99SB-ILDN force field.[38,39] The modeled structures of the liganded and unliganded proteins were each centered in a cubic box and explicitly hydrated with a water layer that extended 10 Å (box size) from the protein surface along each orthogonal direction using the extended simple point charge water model.[40,41] Next, the hydrated structures were energy-minimized with the steepest descent algorithm prior to equilibration under the NPT ensemble conditions, wherein the number of atoms (N), pressure (P), and temperature (T) within the system were kept constant. The Particle-Mesh Ewald method was employed to compute long-range electrostatic interactions with a spherical cutoff of 10 Å and a grid space of 1.6 Å with a fourth order interpolation.[42] The Linear Constraint Solver algorithm was used to restrain bond lengths.[43] All MD simulations were performed at 310 K under periodic boundary condi-

tions, so as to mimic the bulk solvent effect, using the standard "md" leap-frog integrator to solve Newton's equations of motion with a time step of 2 fs. For the final MD production runs, data were collected every ns over a sub-μs time scale. All MD simulations were performed on a Linux workstation using parallel computing at the high-performance computing facility within the Center for Computational Science of the University of Miami. Structural snapshots taken at various intervals during the course of MD simulations were rendered using RIBBONS.[44]

RESULTS AND DISCUSSION

Osmolytes Negatively Regulate the EGR1–DNA Interaction

To understand the effect of osmolytes on EGR1–DNA interaction, we measured the binding of DB domain of EGR1 to ZRE duplex as a function of increasing concentrations of glycerol, sucrose, and PEG400 using ITC. Representative ITC data and binding curves are shown in Figures 2 and 3, while detailed thermodynamics are presented in Tables I and II. Our analysis shows that increasing concentration of osmolytes results in an exponential decrease in the binding affinity, albeit in a differential manner. Thus, while glycerol displays a moderate effect with less than five-fold reduction in binding affinity even when its concentration reaches up to 1000 mM (Figure 3a and Table I), addition of sucrose is concomitant with a drop in affinity by an order of magnitude at a concentration of
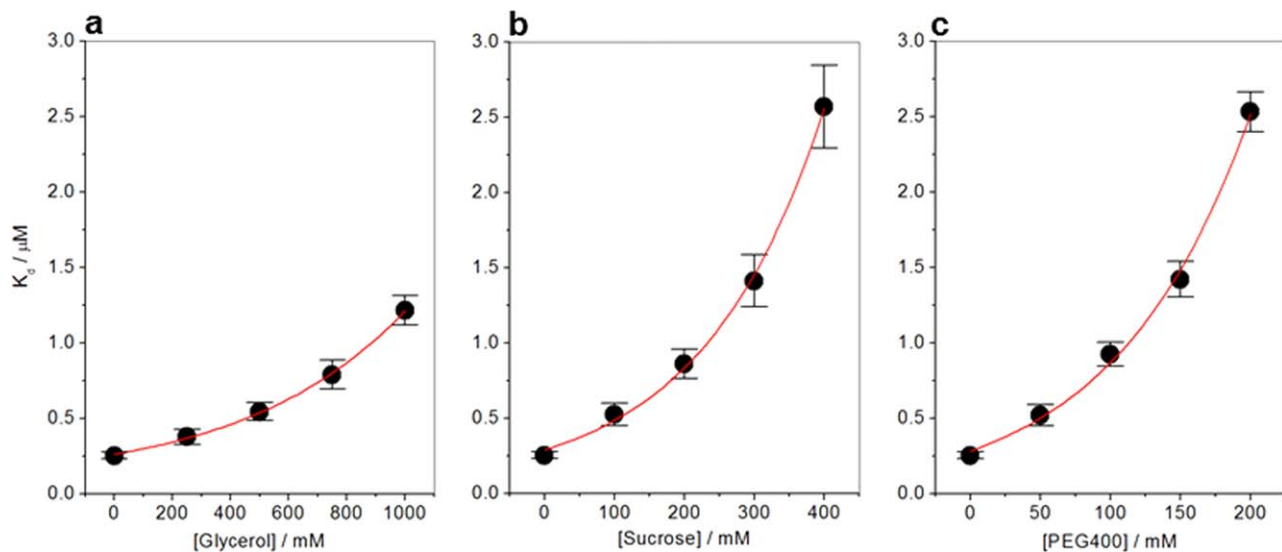
FIGURE 3 Effect of varying concentrations of glycerol (a), sucrose (b), and PEG400 (c) on the apparent equilibrium dissociation constant (K_d) associated with the binding of ZRE duplex to DB domain of EGR1. In all panels, the red solid lines represent exponential fits to data points. The error bars were calculated from at least three independent measurements to one standard deviation.

400 mM (Figure 3b and Table II). In remarkable contrast, PEG400 can achieve a similar feat at only half the concentration of sucrose (Figure 3c and Table III).

Osmolytes are generally believed to stabilize macromolecular conformations and the osmotic stress is expected to aid ligand binding by virtue of its ability to displace water from interacting surfaces.[13–17] The fact that the osmolytes employed here exert an opposite effect on EGR1–DNA interaction strongly argues that they unfavorably interact with EGR1–DNA complex so as to shift the equilibrium in a direction which favors the unliganded conformations. On the other hand, the differential effect of these osmolytes on the binding may be attributed to their ability to differentially interact with the protein and/or DNA and/or due to their differential osmotic effect as a result of their distinct size and chemistry.

Thus, unlike the polyol functionality of glycerol and sucrose, PEG400 is constructed on a polyether backbone. On the other hand, the relatively small size of glycerol (92 g/mol) compared to sucrose (342 g/mol) and PEG400 (400 g/mol) could account for its rather low osmotic potential. Despite their comparable molar mass, the higher osmotic potential of PEG400 suggests that the polyethers are more powerful osmolytes than polyols of comparable molecular size. Additionally, the rather elongated polyether backbone of PEG400 may be better suited to access small cavities and crevices within macromolecules compared to the less accommodating heterocyclic rings of sucrose. Thus, the three-dimensional conformation of osmolytes likely presents an equally important challenge in gauging their osmotic potential and their ability to specifically interact with macromolecules. It is also important to note that the ability of

Table I   Thermodynamic Parameters for the Binding of DB Domain of EGR1 to DNA as a Function of Glycerol Concentration at pH 7.0 and 25°C

[Glycerol] (mM)	K_d (nM)	$\Delta H°$ (kcal.mol^{-1})	$T\Delta S°$ (kcal.mol^{-1})	$\Delta G°$ (kcal.mol^{-1})
0	255 ± 25	−26.93 ± 0.63	−17.92 ± 0.57	−9.01 ± 0.06
250	379 ± 50	−26.29 ± 0.54	−17.52 ± 0.46	−8.77 ± 0.08
500	545 ± 59	−27.2 ± 0.85	−18.65 ± 0.78	−8.56 ± 0.06
750	790 ± 96	−28.33 ± 0.88	−19.99 ± 0.81	−8.34 ± 0.07
1000	1217 ± 97	−29.18 ± 0.63	−21.10 ± 0.67	−8.08 ± 0.05

The binding stoichiometries to the fits agreed to within ±10%. Errors were calculated from at least three independent measurements. All errors are given to one standard deviation.

Table II   Thermodynamic Parameters for the Binding of DB Domain of EGR1 to DNA as a Function of Sucrose Concentration at pH 7.0 and 25°C

[Sucrose] (mM)	K_d (nM)	$\Delta H°$ (kcal.mol^{-1})	$T\Delta S°$ (kcal.mol^{-1})	$\Delta G°$ (kcal.mol^{-1})
0	255 ± 25	−26.93 ± 0.63	−17.92 ± 0.57	−9.01 ± 0.06
100	524 ± 75	−25.93 ± 0.36	−17.37 ± 0.44	−8.58 ± 0.09
200	864 ± 98	−25.28 ± 0.46	−16.99 ± 0.52	−8.28 ± 0.07
300	1413 ± 172	−25.37 ± 0.32	−17.38 ± 0.39	−8.00 ± 0.07
400	2571 ± 273	−25.22 ± 0.51	−17.58 ± 0.57	−7.63 ± 0.06

The binding stoichiometries to the fits agreed to within ±10%. Errors were calculated from at least three independent measurements. All errors are given to one standard deviation.

osmolytes to interact with macromolecules is dependent upon the strength of the cohesive force between the osmolyte and the water solvent.[45–48] In light of our data presented above, it is thus conceivable that the cohesive forces of osmolytes with water decrease in the order PEG400 < sucrose < glycerol and that this reciprocally correlates with their ability to interact with the protein and/or DNA. In other words, the differential ability of osmolytes to mitigate the binding of DB domain to DNA is most probably due to their differential osmophobic effects—the extent to which the osmolytes are excluded from the immediate vicinity of protein surface.[49,50]

Osmolytes Employ Distinct Thermodynamic Mechanisms to Modulate the Binding of EGR1 to DNA

To shed light on how the reduction in binding affinity of DB domain of EGR1 to DNA upon the addition of osmolytes correlates with the contribution of underlying enthalpic ($\Delta H°$) and entropic ($T\Delta S°$) forces to the overall free energy ($\Delta G°$), we constructed various thermodynamic plots (Figure 4). It is evident from such analysis that the osmolytes modulate binding in a thermodynamically distinct manner. Thus, addition of increasing amounts of glycerol results in an increase in the favorable gain of $\Delta H°$ (Figure 4a). However, this favorable enthalpic gain is to a large extent offset by a corresponding

unfavorable gain in $T\Delta S°$ term. On the other hand, $\Delta H°$ term becomes less favorable while $T\Delta S°$ term experiences an opposite trend with increasing concentrations of sucrose (Figure 4b). This behavior is somewhat more exaggerated in the case of PEG400 (Figure 4c), where favorable $\Delta H°$ term undergoes substantial loss with increasing osmolyte concentration while $T\Delta S°$ more or less mirrors an opposite trend. Simply put, the reduction in unfavorable entropic penalty with increasing concentration of PEG400 appears to counteract the loss of favorable enthalpy.

As noted above, one simple interpretation of these differential thermodynamics of EGR1–DNA interaction in the presence of various osmolytes could be ascribed to their ability to differentially interact with the protein and/or DNA due to their differential cohesive forces with water as well as due to their differential osmophobic effects.[45–50] Regardless of the precise physical basis of how these osmolytes interact with the macromolecules, it is clear that the loss or gain of favorable $\Delta H°$ is by and large compensated by an opposite trend in $T\Delta S°$. However, unlike many macromolecular interactions,[51–55] such enthalpy–entropy compensation is not fully obeyed here and thus does not completely eliminate the unfavorable energetic contributions of osmolytes to $\Delta G°$. Indeed, such partial breakdown in $\Delta H° − T\Delta S°$ compensation results in ΔG linearly decreasing with increasing concentration of osmolytes, thereby

Table III   Thermodynamic Parameters for the Binding of DB Domain of EGR1 to DNA as a Function of PEG400 Concentration at pH 7.0 and 25°C

[PEG400] (mM)	K_d (nM)	$\Delta H°$ (kcal.mol^{-1})	$T\Delta S°$ (kcal.mol^{-1})	$\Delta G°$ (kcal.mol^{-1})
0	255 ± 25	−26.93 ± 0.63	−17.92 ± 0.57	−9.01 ± 0.06
50	520 ± 70	−24.16 ± 0.24	−15.58 ± 0.32	−8.58 ± 0.08
100	925 ± 81	−22.88 ± 0.33	−14.57 ± 0.18	−8.24 ± 0.05
150	1423 ± 119	−22.68 ± 0.30	−14.69 ± 0.35	−7.99 ± 0.05
200	2533 ± 131	−22.95 ± 0.19	−15.31 ± 0.16	−7.64 ± 0.03

The binding stoichiometries to the fits agreed to within ±10%. Errors were calculated from at least three independent measurements. All errors are given to one standard deviation.
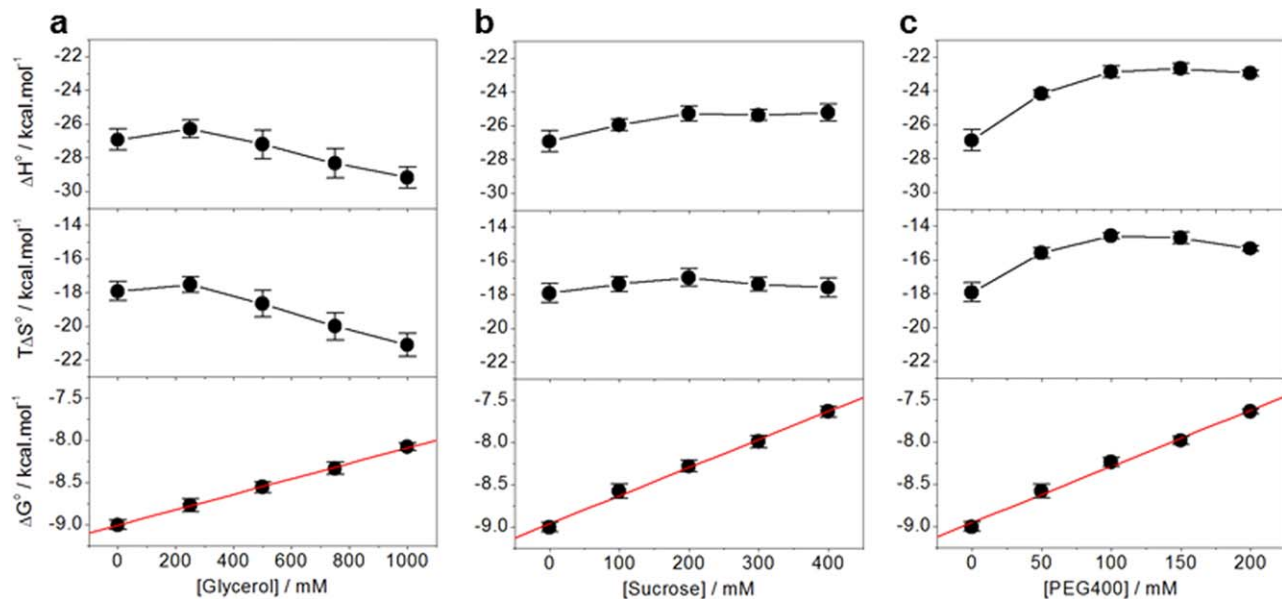
FIGURE 4   Effect of increasing concentrations of glycerol (a), sucrose (b), and PEG400 (c) on enthalpic (ΔH°) and entropic ($T\Delta S^\circ$) contributions to the free energy (ΔG°) accompanying the binding of ZRE duplex to DB domain of EGR1. In the top and middle panels, the solid lines are used to connect data points for clarity. In the bottom panels, the red solid lines represent linear fits to data points. The error bars were calculated from at least three independent measurements to one standard deviation.
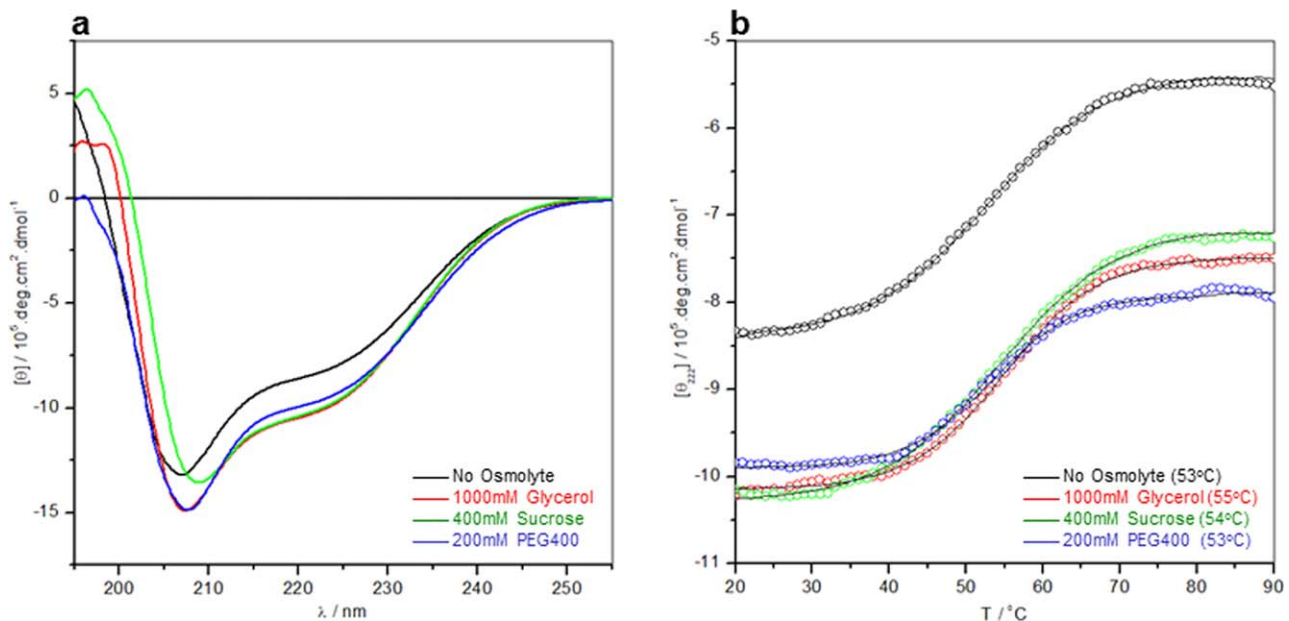

FIGURE 5   Far-UV CD analysis of DB domain of EGR1 in the absence of osmolytes (black) and pre-equilibrated with 1000 m*M* glycerol (red), 400 m*M* sucrose (green), and 200 m*M* PEG400 (blue). (a) Representative far-UV spectra at 25°C. (b) Representative melting curves over the temperature (T) range 20–100°C expressed in terms of the mean ellipticity observed at a wavelength of 222 nm, [θ_{222}]. The solid lines through each dataset represent nonlinear least-squares fits to a two-state model using the ORIGIN software. The values determined for the melting transition (T_m) from these fits under each condition are indicated in the corresponding parenthesis.
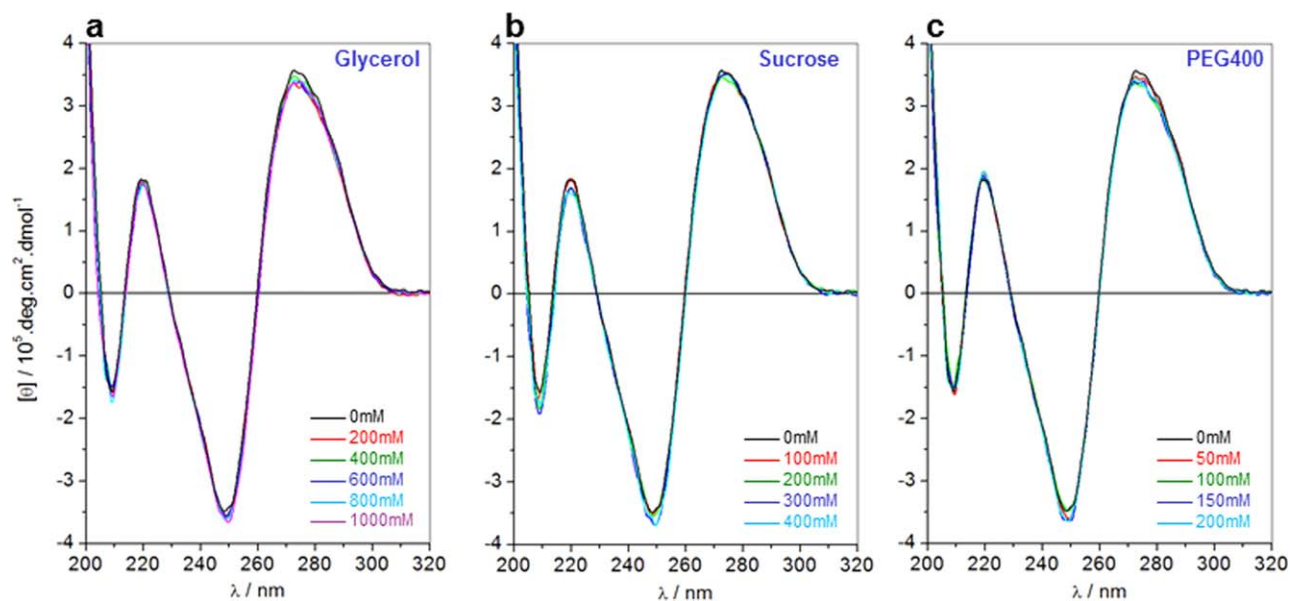
FIGURE 6 Representative CD spectra of ZRE duplex in the absence of osmolytes (black) and pre-equilibrated with varying concentrations of glycerol (a), sucrose (b), and PEG400 (c) as indicated.

accounting for the apparent loss in binding noted above (Tables (I–III)).

Osmolytes Apparently Interact with the DB Domain of EGR1 but Not Its Cognate DNA

In an effort to understand how osmolytes mitigate binding of EGR1 to DNA, we next analyzed the effect of glycerol, sucrose, and PEG400 on the secondary structure and stability of DB domain using far-UV CD analysis (Figure 5). Our data show that the far-UV spectral features of DB domain are largely characterized by a negative band centered around 208 nm with a shoulder at 222 nm due to a mixture of α-helix and β-sheet in agreement with the αβ-fold of the DB domain of EGR1 (Figure 5a). Importantly, the addition of osmolytes appears to perturb the spectral features of DB domain. Thus, the intensity of the 208-nm band along with the 222-nm shoulder undergoes appreciable enhancement in the presence of all three osmolytes. Additionally, the 208-nm band experiences a slight red shift in the presence of sucrose. Together, these observations suggest that the osmolytes stabilize the secondary structure of DB domain to a certain degree, presumably by virtue of their ability to favorably interact with protein backbone atoms.[56] Importantly, the fact that sucrose changes the shape of the spectrum may also imply that it may perturbs the secondary structure of the protein.

Next, to directly probe the effect of various osmolytes on the thermal stability of DB domain, we probed the dependence of mean ellipticity observed at a wavelength of 222nm, $[\theta_{222}]$, in the presence of various osmolytes over the temperature range

20–90°C using far-UV CD (Figure 5b). Surprisingly, our thermal scans suggest that the DB domain displays a melting temperature (T_m) of around 53°C and that the osmolytes apparently have little or negligible effect on T_m. This salient observation suggests that while osmolytes may stabilize the secondary structure of DB domain, this does not translate to any notable change in its overall thermal stability. It is noteworthy that the ability of osmolytes to stabilize protein structure results from the osmophobic effect—the exclusion of osmolytes from the immediate vicinity of protein surface.[49,50] Accordingly, the fact that the osmolytes do not appear to aid thermal stability of DB domain suggests that they stabilize the secondary structure of the unliganded state via favorable interactions. Strikingly, this scenario is in sharp contrast to the ability of osmolytes to promote folding and augment protein stability through their unfavorable interactions with the unfolded state.[13–17] It should however be noted that the relationship between protein structure and stability is of highly subtle nature and the latter is determined by factors other than structure alone. In other words, isostructure does not necessarily equate to isostability. Thus, for example, two proteins with similar thermal stability may harbor substantially different structures and vice versa.

Since osmolytes are generally known to destabilize DNA duplexes,[57,58] we also tested the extent to which glycerol, sucrose and PEG400 may perturb the double-helical character of ZRE duplex using CD analysis (Figure 6). Our data indicate that the ZRE duplex exhibits spectral features characteristic of a right-handed double-stranded B-DNA with a negative band
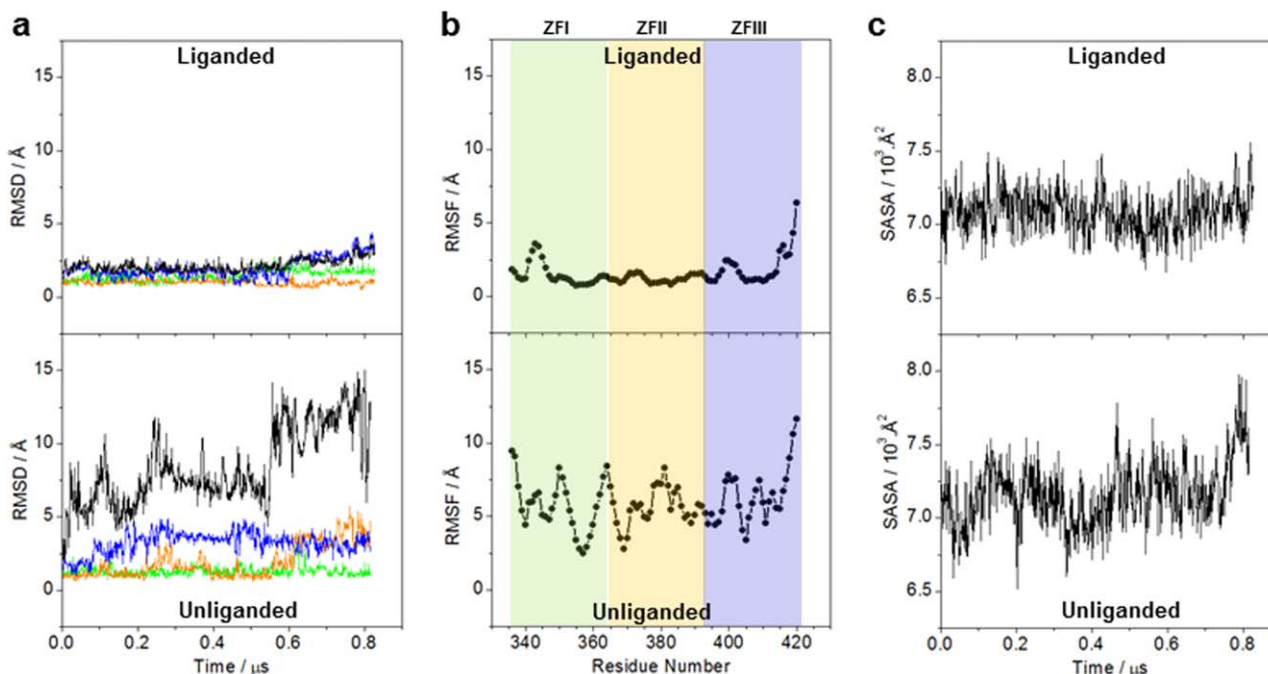
FIGURE 7 Structural stability of EGR1 as probed through MD simulations conducted on the structural models of DB domain bound to DNA (liganded) and in the absence of DNA (unliganded). (a) Root mean square deviation (RMSD) of backbone atoms (N, Cα, and C) within each simulated structure relative to the initial modeled structure of liganded (top panel) and unliganded (bottom panel) protein as a function of simulation time. Note that the overall RMSD of the DB domain (black) is deconvoluted into its three constituent zinc fingers: ZFI (green), ZFII (yellow), and ZFIII (blue). (b) Root mean square fluctuation (RMSF) of backbone atoms (N, Cα, and C) averaged over the entire course of corresponding trajectory of liganded (top panel) and unliganded (bottom panel) protein as a function of residue number. Note that the vertical boxes demarcate the boundaries of ZFI, ZFII, and ZFIII within the DB domain. (c) Solvent-accessible surface area (SASA) of all atoms within each simulated structure relative to the initial modeled structure of liganded (top panel) and unliganded (bottom panel) protein as a function of simulation time.

centered around 250 nm flanked between positive bands centered around 220 and 270 nm. It should be noted here that while the 220-nm band arises from secondary structural DNA features, the 270-nm band probes the three-dimensional conformation of DNA such as bending and curvature. Importantly, the secondary and tertiary structure of ZRE duplex by and large appears to be unaffected in the presence of increasing concentrations of all three osmolytes as monitored by the lack of any notable changes in the shift or intensity of spectral bands (Figures 6a–6c). This strongly argues that the osmolytes employed in this study have little or negligible stabilizing or destabilizing effect on ZRE duplex.

DB Domain of EGR1 Becomes Structurally Destabilized in the Absence of DNA

Although osmolytes do not seem to have any tangible effect on the overall thermal stability of DB domain of EGR1 (Figure

5b), it is nonetheless conceivable that their interaction with the protein—as evidenced by their ability to buttress its secondary structure (Figure 5a)—somehow negatively modulates EGR1–DNA interaction. In particular, the DB domain of EGR1 may be subject to conformational equilibrium such that it fluctuates between multiple conformations in the absence of DNA and undergoes equilibrium shift to a conformation that best fits DNA as noted earlier (Figure 1). Accordingly, the ability of osmolytes to differentially interact with protein conformations that do not best fit DNA could account for the both negative osmotic effect observed here as well as the ability of various osmolytes to buttress the secondary structure of DB domain without altering its overall stability. In order to assess the extent of such conformational space available to the DB domain, we next conducted MD analysis on the protein bound to DNA (liganded) and in the absence of DNA (unliganded) on a sub-μs timescale (Figure 7). Our analysis shows that the liganded DB domain rapidly reaches structural equilibrium
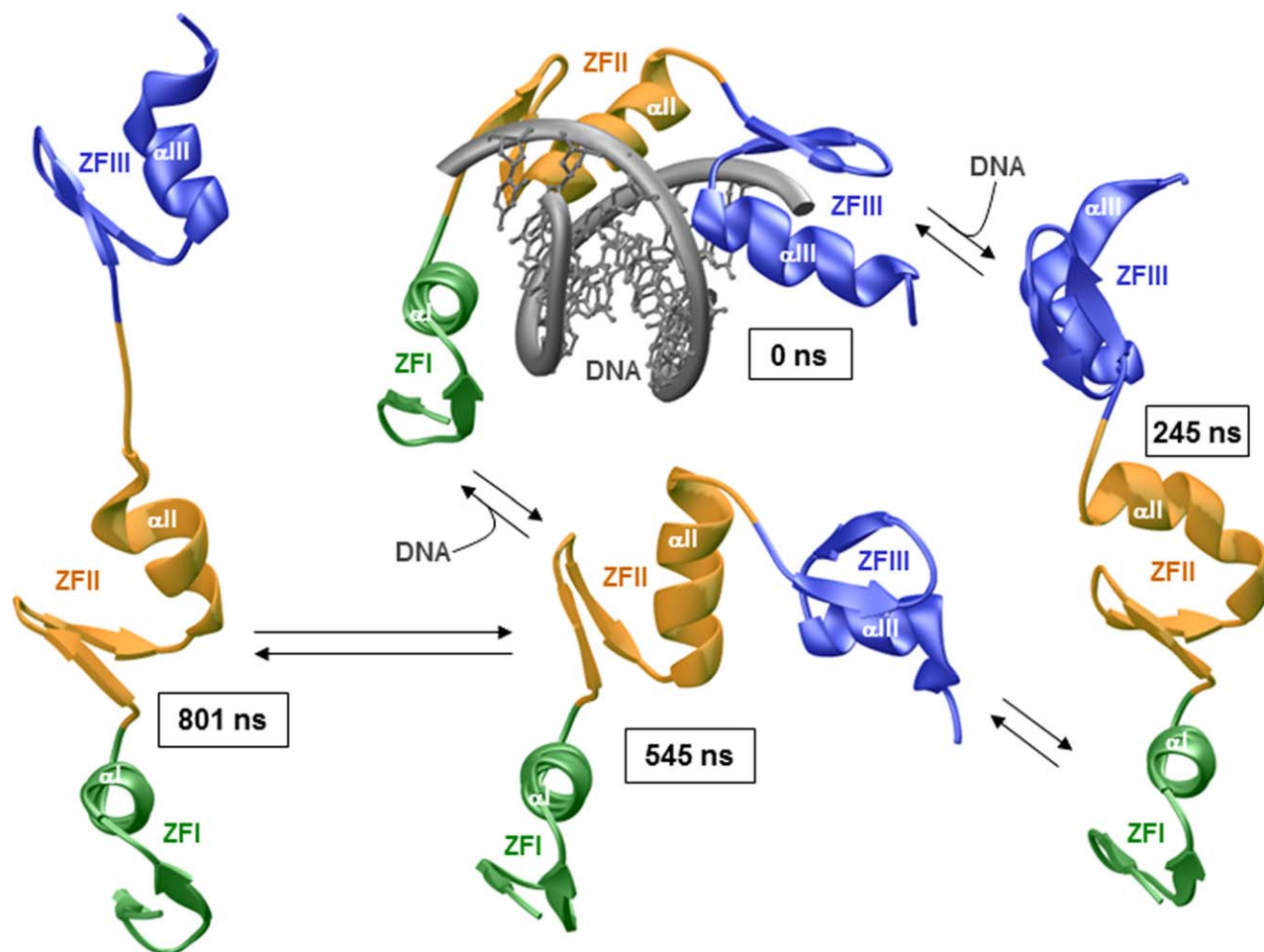
FIGURE 8 Dynamic plasticity of EGR1 as probed through MD simulations conducted on the structural model of DB domain in the absence of DNA (unliganded). Shown are structural snapshots taken at 0, 245, 545, and 801 ns during the course of an MD simulation. The three tandem zinc fingers constituting the DB domain are colored green (ZFI), yellow (ZFII), and blue (ZFIII) and the coordinating zinc divalent ions have been eliminated for clarity. Note that the DNA (colored gray) bound to the 0-ns snapshot is stripped away at the start of MD simulation and is only shown here for comparison.

with a root mean square deviation (RMSD) for the backbone atoms of around 2 Å (Figure 7a). In remarkable contrast, the unliganded protein does not appear to attain a structural equilibrium over the course of entire simulation and continues to display rather large deviations or oscillations comprised of periodic peaks reaching as high as 14 Å and troughs touching as low as 4 Å. Importantly, the motional behavior of the unliganded protein resembles a wave-like form with a period in the order of hundreds of ns, which corresponds to a resonance frequency in the MHz regime, accompanied by an amplitude approaching 5 Å. Such resonant behavior is indicative of the fact that the DB domain samples a rather large conformational space between two well-defined states that occupy the energy minima at each extreme of this structural landscape (corresponding to the peaks and troughs on the trajectory).

In an attempt to unearth the origin of such dynamic behavior, we deconvoluted the overall RMSD of the DB domain into its three constituent zinc fingers, namely ZFI, ZFII, and ZFIII (Figure 7a). In the case of liganded protein, ZFI and ZFII appear to be relatively stable, while ZFIII largely resembles the dynamics of the DB domain. This suggests that the structural deviation of liganded DB domain mentioned above is largely attributable to ZFIII. On the other hand, while ZFI appears to be relatively stable in the unliganded protein, ZFII and ZFIII are much less stable, implying that they predominantly contribute to the dynamics of the unliganded conformation noted above. In particular, the role of zinc fingers in imparting structural flexibility upon the unliganded DB domain appears to be polarized with the mobility of the N-terminal ZFI being

relatively muted, while the central ZFII becoming structurally destabilized and such instability particularly bearing heavily upon ZFIII. Consistent with these observations, our root mean square fluctuation analysis reveals that while the backbone dynamics of most residues within the unliganded protein are significantly perturbed relative to their counterparts in the liganded protein, the C-terminal residues spanning ZFIII display somewhat similar dynamic profile in both cases (Figure 7b). This salient observation implies that the C-terminal region of DB domain harbors intrinsic flexibility, which fires off a domino-like effect on rest of the protein when DNA is pulled out of the union. Next, we also compared the extent of solvent-accessible surface area (SASA) in both the liganded and unliganded forms of DB domain of EGR1 as a function of simulation time (Figure 7c). Unsurprisingly, residues within the rod-like unliganded protein on average appear to be more solvated than their counterparts in the liganded form. This observation thus clearly suggests that the osmolytes ought to enhance rather than mitigate the binding of DB domain of EGR1 to DNA by virtue of their ability to displace water from the unliganded state. However, the fact that the opposite trend is observed here supports the notion that the osmolytes likely engage in specific interactions with the unliganded conformation of EGR1 and mitigate its ability to bind DNA.

DB Domain of EGR1 Undergoes Equilibrium Shift Upon Binding to DNA

Our data presented above suggest that the unliganded DB domain of EGR1 is in equilibrium exchange between two distinct states that periodically interconvert on a time scale in the order of hundreds of ns. The contemporary view of ligand binding holds that in the absence of ligand, structurally flexible proteins sample multiple conformations, one of which best fits the ligand.[59–61] In this so-called equilibrium shift model, ligand binding to this preformed conformation simply shifts the equilibrium in its direction in lieu of the ligand directly inducing structural changes necessary for its accommodation within the host protein. Could one of the two distinct states of the DB domain observed in our MD simulations represent the preformed conformation proposed in the equilibrium shift model? If so, what is the physical nature of the other conformation that it is in equilibrium exchange with?

To address these tantalizing issues, we took structural snapshots of the unliganded DB domain at simulation times of 245 ns (peak), 545 ns (trough), and 801 ns (peak), corresponding to intermittent peaks and troughs observed in the RMSD trajectory (Figure 7a), and compared these interconverting species to the initial or starting structure from which the DNA has been forcibly stripped away (0 ns) during the course of simula-

tion cycle. As shown in Figure 8, the three tandem zinc fingers (ZFI, ZFII, and ZFIII) come together and impart upon the DB domain an arc-like conformation best suited to allow them to tightly snuggle into the major grooves of DNA in a cooperative manner. However, in the 245-ns snapshot (corresponding to a peak in the RMSD trajectory), ZFIII appears to flip out by more than 90° about an axis through ZFI and ZFII such that the resulting collinear orientation of the three zinc fingers allows the DB domain to adopt a rod-like shape. Such conformational change would clearly favor dissociation of the protein from DNA and vice versa. It is also noteworthy that in addition to collinear rearrangement of the three zinc fingers within the DB domain, the C-terminal α-helices of ZFII (αII) and ZFIII (αIII) undergo partial unwinding resulting in the loss of helicity by about one turn. Thus, the DB domain not only experiences tertiary but also secondary structural changes in the absence of DNA. It is thus conceivable that the osmolytes facilitate the folding of these partially unstructured α-helices in the unliganded conformation but, in so doing, also hinder its ability to undergo exchange to an arc-like conformation best suited to bind DNA (Figure 5a).

Most significantly, the 545-ns snapshot (corresponding to a trough in the RMSD trajectory) reveals that the conformation adopted by the DB domain at this time point during the course of simulation very much resembles that of the liganded protein bound to DNA (0-ns snapshot). On the other hand, the 801-ns snapshot reveals that the unliganded protein becomes even more extended than the rod-like shape observed at 245 ns. Together, these data strongly argue that the unliganded DB domain is in equilibrium exchange between two well-defined states, an extended rod-like state and an arc-like preformed conformation that best fits the ligand as proposed in the equilibrium shift model.[59–61] In light of these observations, we believe that the osmolytes favorably interact with the rod-like unliganded state and thereby render it less favorable to undergo conformational exchange to an arc-like conformation best suited to fit DNA. Importantly, such a scenario would not only account for the ability of osmolytes to mitigate the binding of EGR1 to DNA but could also explain their ability to stabilize the secondary structure of the unliganded protein without aiding its thermal stability as observed in our CD measurements (Figure 5). Thus, for example, the rod-like state of protein would offer maximal surface area for the favorable interactions with osmolytes and the higher the concentration of osmolytes the greater the population of the rod-like state. In contrast, the rather arc-like conformation that the protein adopts in the liganded state would sterically hamper its interaction with osmolytes even though such protein–osmolyte interactions may not

necessarily be unfavorable. In this regard, the ease with which osmolytes may be able to favorably interact with the rod-like unliganded state would incur a thermodynamic penalty upon their exclusion from the protein surface so as to enable the binding of DNA. Comparison of SASA values for various interconverting conformational states indeed further corroborate this notion (Figure 7c). More specifically, while SASA for the rod-like state observed at 801 ns is calculated to be 7719 $\mathrm{\mathring{A}}^2$, a much smaller value of 6835 $\mathrm{\mathring{A}}^2$ is obtained for the arc-like conformation best suited to fit DNA. In short, the osmolytes likely shift the equilibrium in the direction of the rod-like unliganded state that is poorly suited to fit DNA and, in so doing, mitigate the EGR1–DNA interaction.

CONCLUSION

Addition of osmolytes to an aqueous solution of macromolecules introduces osmotic stress—a phenomenon that results in molecular crowding leading to an increase in the effective concentration of all species but a decrease in their entropic freedom. Accordingly, the osmotic stress should in principle be expected to favor macromolecular activities such as ligand binding and enzymatic activity by virtue of not only augmenting the collisional probability between the interacting species (kinetic advantage) but also through reduction of entropy of free species so as to facilitate their association (thermodynamic advantage). However, another important virtue of osmotic stress is that it also displaces water from macromolecular surfaces such that processes that involve the net release of water into the bulk solvent will be favored, while those that involve net uptake would be subject to inhibition.[62–66] As a consequence, water is believed to play an active role in mediating many macromolecular interactions by virtue of its ability to shift conformational exchange between distinct states through coupled hydration–dehydration equilibria.[67–69] Thus, hemoglobin sequesters more than 50 waters upon loading oxygen,[67] the opening of ionic channel alamethicin is coupled to a net uptake of 100 waters,[70] and the pyrimidine biosynthesis pathway workhorse aspartate transcarbamylase gulps over 200 waters upon substrate binding.[71] On the other hand, binding of TBP and CAP proteins to their cognate promoters results in the expulsion of tens of waters,[72,73] interaction of EcoR1 and BamH1 restriction endonucleases with DNA ejects over 100 waters,[74–76], the binding of lac repressor to its promoter is concomitant with the net release of over 200 waters,[77] and hexokinase may part company with as many as 300 waters when called upon to phosphorylate glucose during the first step of glycolysis.[68,69]

Notably, our analysis on EGR1–DNA interaction presented here suggests that the rod-like unliganded protein is likely to be more hydrated than the arc-like liganded conformation that best fits DNA. Thus, it is unlikely that the reduction in the binding of EGR1 to DNA in the presence of osmolytes could be accounted in terms of the coupling of water uptake. On the contrary, our study suggests that the osmolytes favorably interact with the rod-like unliganded state and thereby render it less favorable to undergo conformational exchange to an arc-like state best suited to bind DNA. Indeed, preferential interactions of osmolytes with proteins and their ability to shift conformational equilibria are well documented. For example, proline binds to the folding intermediate of lysozyme so as to not only promote its refolding but also prevent aggregation.[78] Consistent with this observation, proline along with other natural osmolytes such as glycerol and heparin promote the refolding of creatine kinase by virtue of their ability to favorably interact with folding intermediates, thereby shifting the equilibrium in the direction of the native state in lieu of protein aggregation.[79] A similar effect of proline is also observed on P39A cellular retinoic-acid binding protein.[80] Other studies suggest that proline at high concentration aids the solubility of proteins via favorable interactions.[81] On the other hand, the favorable interaction of methylamines such as TMG, NMG, and TMAO with monomeric conformations of serpins inhibits their disease-causing polymerization.[82] While osmolytes in general prevent aggregation of globular proteins, they exhibit an opposite effect on intrinsically disordered proteins (IDPs). Thus, for example, the intrinsically disordered α-synuclein, a protein implicated in the development of Parkinson's disease, undergoes aggregation into an heterogeneous ensemble of oligomers and amyloid-like fibrils in the presence of a variety of osmolytes.[83–85] More importantly, such osmolyte-induced aggregation and fibrillation of α-synuclein has also been reported in the case of several other IDPs such as the microtubule-associated protein tau,[86] *S*-carboxymethylated α-lactalbumin,[87] the prion protein,[88] the glucagon hormone peptide,[89] and Alzheimer's amyloid-β peptides.[90–92]

It is noteworthy that proteins under physiological conditions do not usually adopt a well-defined state but rather an ensemble of rapidly interconverting conformations primed to quickly allow the protein to switch its function depending on the nature of biological stimulus. Importantly, such conformational equilibria in proteins are highly sensitive to varying concentrations of osmolytes,[93] which are believed to preferentially bind to specific conformational states over others. In particular, it has been shown that osmolytes such as methylamines modulate a highly cooperative structural transition in the Hsp90 chaperone between an open and closed conformation that only differ by a domain–domain interaction.[94] It is striking to note that while Hsp90 adopts an additional ATP-bound state, this conformation appears to be more or less resistant to

varying concentrations of osmolytes. This suggests that the preferential interactions of osmolytes with proteins may also play a key role in maintaining their conformational heterogeneity in a manner akin to their ability to promote protein stability. It should also be noted here that the interaction of osmolytes are not only restricted to water-soluble proteins. For example, substrate binding triggers unfolding of the N-terminal region of BtuB membrane transporter, while osmolytes such as PEGs and methylamines inhibit such order–disorder transition by virtue of their ability to specifically interact with the folded conformation.[95,96] Notably, increasing the molecular size of PEGs beyond about 2000 g/mol leads to little or no further increase in the excluded volume of water in Btu, implying that the larger osmolytes are preferentially excluded from accessing specific cavities within the protein.

While precise mechanism of how osmolytes exert their such a diverse array of effect on macromolecules remain largely obscure, our demonstration that they negatively modulate EGR1–DNA interaction bears important therapeutic implications. Thus, for example, osmolytes could be therapeutically exploited to down-regulate the oncogenic potential of EGR1 and other related transcription factors. Indeed, the use of osmolytes to hinder protein misfolding and aggregation has been suggested to be an important therapeutic tool to alleviate many pathological and neurodegenerative disorders.[21] In sum, our study not only provides new insights into the effect of osmolytes on a key protein-DNA interaction but also warrants further investigations into the role of osmolytes in regulating the biological activity of transcription factors.

ACKNOWLEDGMENTS

REFERENCES

1. Yancey, P. H. Sci Prog 2004, 87, 1–24.
2. Yancey, P. H.; Rhea, M. D.; Kemp, K. M.; Bailey, D. M. Cell Mol Biol (Noisy-le-grand) 2004, 50, 371–376.
3. Yancey, P. H. J Exp Biol 2005, 208, 2819–2830.
4. Yancey, P. H.; Clark, M. E.; Hand, S. C.; Bowlus, R. D.; Somero, G. N. Science 1982, 217, 1214–1222.
5. Baskakov, I.; Bolen, D. W. J Biol Chem 1998, 273, 4831–4834.
6. Mello, C. C.; Barrick, D. Protein Sci 2003, 12, 1522–1529.
7. Baskakov, I.; Wang, A.; Bolen, D. W. Biophys J 1998, 74, 2666–2673.
8. Holthauzen, L. M.; Bolen, D. W. Protein Sci 2007, 16, 293–298.
9. Wang, A.; Bolen, D. W. Biochemistry 1997, 36, 9101–9108.
10. Singh, L. R.; Dar, T. A.; Rahman, S.; Jamal, S.; Ahmad, F. Biochim Biophys Acta 2009, 1794, 929–935.
11. Rosgen, J.; Pettitt, B. M.; Bolen, D. W. Biophys J 2005, 89, 2988–2997.
12. Bolen, D. W. Methods 2004, 34, 312–322.
13. Qu, Y.; Bolen, C. L.; Bolen, D. W. Proc Natl Acad Sci USA 1998, 95, 9268–9273.
14. Bolen, D. W. Methods Mol Biol 2001, 168, 17–36.
15. Bolen, D. W.; Baskakov, I. V. J Mol Biol 2001, 310, 955–963.
16. Wu, P.; Bolen, D. W. Proteins 2006, 63, 290–296.
17. Lin, T. Y.; Timasheff, S. N. Biochemistry 1994, 33, 12695–12701.
18. Auton, M.; Ferreon, A. C.; Bolen, D. W. J Mol Biol 2006, 361, 983–992.
19. Auton, M.; Rosgen, J.; Sinev, M.; Holthauzen, L. M.; Bolen, D. W. Biophys Chem 2011, 159, 90–99.
20. Linhananta, A.; Hadizadeh, S.; Plotkin, S. S. Biophys J 2011, 100, 459–468.
21. Singh, L. R.; Poddar, N. K.; Dar, T. A.; Kumar, R.; Ahmad, F. Life Sci 2011, 88, 117–125.
22. Gashler, A.; Sukhatme, V. P. Prog Nucleic Acid Res Mol Biol 1995, 50, 191–224.
23. Sukhatme, V. P. J Am Soc Nephrol 1990, 1, 859–866.
24. Christy, B. A.; Lau, L. F.; Nathans, D. Proc Natl Acad Sci USA 1988, 85, 7857–7861.
25. Christy, B.; Nathans, D. Proc Natl Acad Sci USA 1989, 86, 8737–8741.
26. Pavletich, N. P.; Pabo, C. O. Science 1991, 252, 809–817.
27. Yan, S. F.; Fujita, T.; Lu, J.; Okada, K.; Shan Zou, Y.; Mackman, N.; Pinsky, D. J.; Stern, D. M. Nat Med 2000, 6, 1355–1361.
28. Thiel, G.; Cibelli, G. J Cell Physiol 2002, 193, 287–292.
29. Ahmed, M. M. Curr Cancer Drug Targets 2004, 4, 43–52.
30. Adamson, E. D.; Mercola, D. Tumour Biol 2002, 23, 93–102.
31. Mikles, D. C.; Bhat, V.; Schuchardt, B. J.; Deegan, B. J.; Seldeen, K. L.; McDonald, C. B.; Farooq, A. FEBS J 2013, 280, 3669–3684.
32. Gasteiger, E.; Hoogland, C.; Gattiker, A.; Duvaud, S.; Wilkins, M. R.; Appel, R. D.; Bairoch, A. In The Proteomics Protocols Handbook; Walker, J. M., Ed., Chapter 52; Humana Press: Totowa, NJ, 2005; pp 571–607.
33. Wiseman, T.; Williston, S.; Brandts, J. F.; Lin, L. N. Anal Biochem 1989, 179, 131–137.
34. Marti-Renom, M. A.; Stuart, A. C.; Fiser, A.; Sanchez, R.; Melo, F.; Sali, A. Annu Rev Biophys Biomol Struct 2000, 29, 291–325.
35. Koradi, R.; Billeter, M.; Wuthrich, K. J Mol Graph 1996, 14, 51–55.
36. Van Der Spoel, D.; Lindahl, E.; Hess, B.; Groenhof, G.; Mark, A. E.; Berendsen, H. J. J Comput Chem 2005, 26, 1701–1718.
37. Hess, B. J Chem Theory Comput 2008, 4, 435–447.
38. Lindorff-Larsen, K.; Piana, S.; Palmo, K.; Maragakis, P.; Klepeis, J. L.; Dror, R. O.; Shaw, D. E. Proteins 2010, 78, 1950–1958.
39. Hornak, V.; Abel, R.; Okur, A.; Strockbine, B.; Roitberg, A.; Simmerling, C. Proteins 2006, 65, 712–725.
40. Toukan, K.; Rahman, A. Phys Rev B 1985, 31, 2643–2648.
41. Berendsen, H. J. C.; Grigera, J. R.; Straatsma, T. P. J Phys Chem 1987, 91, 6269–6271.
42. Darden, T. A.; York, D.; Pedersen, L. J Chem Phys 1993, 98, 10089–10092.
43. Hess, B.; Bekker, H.; Berendsen, H. J. C.; Fraaije, J. G. E. M. J Comput Chem 1997, 18, 1463–1472.
44. Carson, M. J Appl Crystallogr 1991, 24, 958–961.

45. Lee, J. C.; Timasheff, S. N. J Biol Chem 1981, 256, 7193–7201.

46. Gekko, K.; Timasheff, S. N. Biochemistry 1981, 20, 4667–4676.

47. Vagenende, V.; Yap, M. G.; Trout, B. L. Biochemistry 2009, 48, 11084–11096.

48. Vagenende, V.; Yap, M. G.; Trout, B. L. J Phys Chem B 2009, 113, 11743–11753.

49. Timasheff, S. N. Biochemistry 2002, 41, 13473–13482.

50. Timasheff, S. N. Proc Natl Acad Sci USA 2002, 99, 9721–9726.

51. Lumry, R.; Rajender, S. Biopolymers 1970, 9, 1125–1227.

52. Eftink, M. R.; Anusiem, A. C.; Biltonen, R. L. Biochemistry 1983, 22, 3884–3896.

53. Cooper, A.; Johnson, C. M.; Lakey, J. H.; Nollmann, M. Biophys Chem 2001, 93, 215–230.

54. Sharp, K. Protein Sci 2001, 10, 661–667.

55. Starikov, E. B.; Norden, B. J Phys Chem B 2007, 111, 14431–14435.

56. Street, T. O.; Bolen, D. W.; Rose, G. D. Proc Natl Acad Sci USA 2006, 103, 13997–14002.

57. Rajendrakumar, C. S.; Suryanarayana, T.; Reddy, A. R. FEBS Lett 1997, 410, 201–205.

58. Rees, W. A.; Yager, T. D.; Korte, J.; von Hippel, P. H. Biochemistry 1993, 32, 137–144.

59. Kumar, S.; Ma, B.; Tsai, C. J.; Sinha, N.; Nussinov, R. Protein Sci. 2000, 9, 10–19.

60. Tsai, C.-J.; Ma, B.; Nussinov, R. Proc Natl Acad Sci USA 1999, 96, 9970–9972.

61. Ma, B.; Kumar, S.; Tsai, C.-J.; Nussinov, R. Protein Eng 1999, 12, 713–720.

62. Rand, R. P.; Parsegian, V. A.; Rau, D. C. Cell Mol Life Sci 2000, 57, 1018–1032.

63. Parsegian, V. A.; Rand, R. P.; Rau, D. C. Proc Natl Acad Sci USA 2000, 97, 3987–3992.

64. Rand, R. P. Philos Trans R Soc Lond B Biol Sci 2004, 359, 1277–1284; discussion 1284-1275.

65. Parsegian, V. A.; Rand, R. P.; Rau, D. C. Methods Enzymol 1995, 259, 43–94.

66. Leikin, S.; Parsegian, V. A.; Rau, D. C.; Rand, R. P. Annu Rev Phys Chem 1993, 44, 369–395.

67. Colombo, M. F.; Rau, D. C.; Parsegian, V. A. Science 1992, 256, 655–659.

68. Reid, C.; Rand, R. P. Biophys J 1997, 72, 1022–1030.

69. Rand, R. P.; Fuller, N. L.; Butko, P.; Francis, G.; Nicholls, P. Biochemistry 1993, 32, 5925–5929.

70. Vodyanoy, I.; Bezrukov, S. M.; Parsegian, V. A. Biophys J 1993, 65, 2097–2105.

71. LiCata, V. J.; Allewell, N. M. Biochemistry 1997, 36, 10161–10167.

72. Khrapunov, S.; Brenowitz, M. Biophys J 2004, 86, 371–383.

73. Vossen, K. M.; Wolz, R.; Daugherty, M. A.; Fried, M. G. Biochemistry 1997, 36, 11640–11647.

74. Lynch, T. W.; Sligar, S. G. J Biol Chem 2000, 275, 30561–30565.

75. Sidorova, N. Y.; Rau, D. C. Proc Natl Acad Sci USA 1996, 93, 12272–12277.

76. Sidorova, N. Y.; Muradymov, S.; Rau, D. C. J Biol Chem 2006, 281, 35656–35666.

77. Fried, M. G.; Stickle, D. F.; Smirnakis, K. V.; Adams, C.; MacDonald, D.; Lu, P. J Biol Chem 2002, 277, 50676–50682.

78. Samuel, D.; Kumar, T. K.; Ganesh, G.; Jayaraman, G.; Yang, P. W.; Chang, M. M.; Trivedi, V. D.; Wang, S. L.; Hwang, K. C.; Chang, D. K.; Yu, C. Protein Sci 2000, 9, 344–352.

79. Meng, F.; Park, Y.; Zhou, H. Int J Biochem Cell Biol 2001, 33, 701–709.

80. Ignatova, Z.; Gierasch, L. M. Proc Natl Acad Sci USA 2006, 103, 13357–13361.

81. Samuel, D.; Kumar, T. K.; Jayaraman, G.; Yang, P. W.; Yu, C. Biochem Mol Biol Int 1997, 41, 235–242.

82. Chow, M. K.; Devlin, G. L.; Bottomley, S. P. Biol Chem 2001, 382, 1593–1599.

83. Uversky, V. N.; Li, J.; Fink, A. L. FEBS Lett 2001, 509, 31–35.

84. Munishkina, L. A.; Henriques, J.; Uversky, V. N.; Fink, A. L. Biochemistry 2004, 43, 3289–3300.

85. Munishkina, L. A.; Cooper, E. M.; Uversky, V. N.; Fink, A. L. J Mol Recogn 2004, 17, 456–464.

86. Scaramozzino, F.; Peterson, D. W.; Farmer, P.; Gerig, J. T.; Graves, D. J.; Lew, J. Biochemistry 2006, 45, 3684–3691.

87. Bomhoff, G.; Sloan, K.; McLain, C.; Gogol, E. P.; Fisher, M. T. Arch Biochem Biophys 2006, 453, 75–86.

88. Nandi, P. K.; Bera, A.; Sizaret, P. Y. J Mol Biol 2006, 362, 810–820.

89. Macchi, F.; Eisenkolb, M.; Kiefer, H.; Otzen, D. E. Int J Mol Sci 2012, 13, 3801–3819.

90. Fung, J.; Darabie, A. A.; McLaurin, J. Biochem Biophys Res Commun 2005, 328, 1067–1072.

91. Yang, D. S.; Yip, C. M.; Huang, T. H.; Chakrabartty, A.; Fraser, P. E. J Biol Chem 1999, 274, 32970–32974.

92. Kim, H. Y.; Kim, Y.; Han, G.; Kim, D. J. J Alzheimers Dis 2010, 22, 73–85.

93. Lopez, C. J.; Fleissner, M. R.; Guo, Z.; Kusnetzow, A. K.; Hubbell, W. L. Protein Sci 2009, 18, 1637–1652.

94. Street, T. O.; Krukenberg, K. A.; Rosgen, J.; Bolen, D. W.; Agard, D. A. Protein Sci 2010, 19, 57–65.

95. Fanucci, G. E.; Lee, J. Y.; Cafiso, D. S. Biochemistry 2003, 42, 13106–13112.

96. Kim, M.; Xu, Q.; Fanucci, G. E.; Cafiso, D. S. Biophys J 2006, 90, 2922–2929.

Reviewing Editor: Kenneth J. Breslauer